Journal of Vibration and Control

http://jvc.sagepub.com

Applicability of Attractor Control Techniques for a Particle Conveyed by a Propagating Wave

M. Ragulskis and K. Koizumi

Journal of Vibration and Control 2004; 10; 1057
DOI: 10.1177/1077546304041189

Applicability of Attractor Control Techniques for a Particle Conveyed by a Propagating Wave

M. RAGULSKIS
Department of Mathematical Research in Systems, Kaunas University of Technology, Kaunas, Lithuania

K. KOIZUMI
Department of Pathogenic Biochemistry, Toyama University, Toyama, Japan

(Received 3 February 2003; accepted 14 October 2003)

Abstract: The governing equations of motion describing the dynamics of a conveyed particle by a propagating surface wave are derived. Although the problem may look rather primitive, it holds considerable complications first of all due to the fact that the shape of the surface cannot be described explicitly. Special forward and reverse time marching numerical techniques, incorporating the solution of nonlinear algebraic equations in every time step, are developed for time integration of derived differential equations. It is shown that the described system possesses numerous nonlinear features such as sensitivity to initial conditions, coexisting attractors. This fact builds the foundation for the potential applicability of attractor control techniques based on small external impulses.

Key Words: Propagating wave, attractor, nonlinear dynamics

1. INTRODUCTION

Mechanical transportation of particles by propagating waves is an important engineering problem with numerous applications. The basic principle of such conveyance is exploited in many different systems such as vibration conveyors, longitudinal or angular ultrasonic motors, vibration feeders, etc. Although the mathematical modeling of such systems may look rather primitive, the derivation of the governing equations of motion faces considerable complications. This paper is focused on the construction of a model of a conveyed particle and the investigation of its nonlinear dynamics when the amplitude of the propagating wave is not small.

2. BACKGROUND

Whenever a traveling surface wave occurs in a medium, it can be characterized by a retrograde elliptic motion of the particles of the media. Typical examples could be a traveling Rayleigh wave in an elastic medium, or water waves (deep or shallow) without mass transport. When

Journal of Vibration and Control, **10:** 1057–1070, 2004 DOI: 10.1177/1077546304041189

the amplitude of the propagating wave is small, the instantaneous shape of the boundary of the media can be approximated as a harmonic function. When the amplitude of the wave is not small, the motion of the particles of the media is still elliptic, but the shape of the boundary is not harmonic (Achenbach, 1984; Landau and Lifschitz, 1986). Although there have been numerous attempts devoted to the analysis of the dynamics of a particle conveyed by a propagating wave (Tokar and Ulitko, 1984; Jacobsen et al., 1994; Benisti and Escande, 1997; Elskens et al., 1998; Hui and Tomita, 2000), all of these incorporate some sort of simplification. Accurate modeling of even such apparently simple dynamical system faces considerable complications due to the fact that the instantaneous shape of the boundary (profile) cannot be described explicitly. This can be illustrated by kinematic relationships describing a traveling Rayleigh wave.

Explicitly, the longitudinal and transverse displacements of the medium at the surface of the flat boundary with a traveling Rayleigh wave can be expressed as a harmonic (Achenbach, 1984; Landau and Lifschitz, 1986)

$$\begin{aligned} u_x &= \frac{\omega}{\chi}\sqrt{\frac{2\rho\,(1+v)}{E}}\left(1-\frac{\sqrt{1-\chi^2}\sqrt{2\,(1-v)-\chi^2\,(1-2v)}}{(1-0,5\chi^2)\sqrt{2\,(1-v)}}\right)C\sin\left(\omega t\mp kx\right); \\ u_y &= \frac{\omega}{\chi}\sqrt{\frac{2\rho\,(1+v)}{E}}\left(1-\frac{\sqrt{2\,(1-v)-\chi^2\,(1-2v)}}{\sqrt{2\,(1-v)}}\right)0,5\chi^2 C\cos\left(\omega t\mp kx\right), \end{aligned} \quad (1)$$

where u_x and u_y are longitudinal and transverse displacements, x is the coordinate of the surface point of the medium before the wave process takes place, C is const, k is the wavenumber, and ρ is the density. χ can be found from the following algebraic equation (Achenbach, 1984)

$$\chi^6-8\chi^4+8\left(3-\frac{1-2v}{1-v}\right)\chi^2-16\left(1-\frac{1-2v}{2\,(1-v)}\right)=0, \quad (2)$$

and angular velocity ω can be found from the following transcendental equation (Achenbach, 1984)

$$\left(k^2+\beta^2\right)^2\cosh\left(\alpha a\right)\sinh\left(\beta a\right)-4k^2\alpha\beta\cosh\left(\beta a\right)\sinh\left(\alpha a\right)=0, \quad (3)$$

where $\alpha=\sqrt{\frac{v_l k^2-\omega^2}{v_l^2}}$, $\beta=\sqrt{\frac{v_t k^2-\omega^2}{v_t^2}}$, $v_l=\sqrt{\frac{\lambda+2\mu}{\rho}}$, $v_t=\sqrt{\frac{\mu}{\rho}}$, v is the Poisson ratio, and λ is the first Lamé constant.

It can be noted that the ratio between the amplitudes of transverse and longitudinal deformations depends on v. In usual elastic media, it is quite normal that the transverse displacement is about 1.5 times larger than the longitudinal displacement (Landau and Lifschitz, 1986). The motion of a point in the medium is an ellipse. Also, the direction of the velocity of the particles at the peaks of the wave is opposite to the direction of wave propagation. Particle displacements are greatest at the surface and decrease exponentially downward.

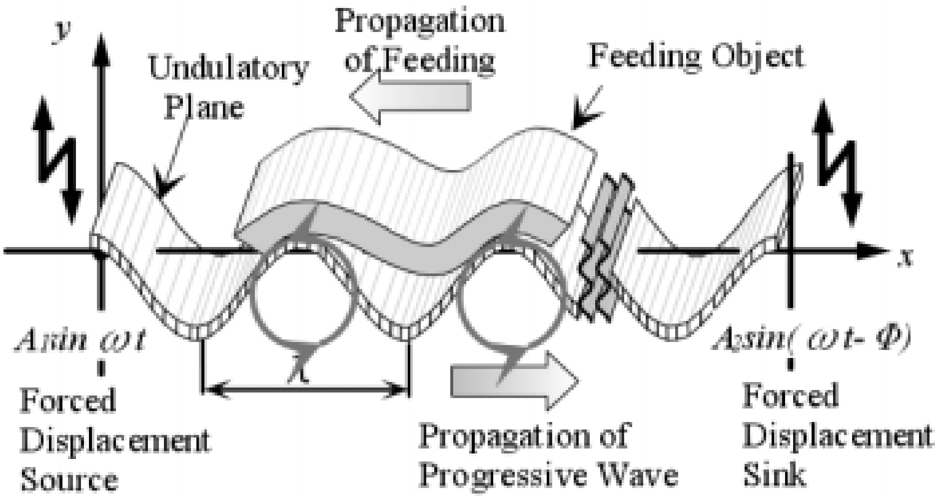

Figure 1. Schematic diagram of a film-feeding instrument.

3. GEOMETRY OF THE PROFILE AND CONSTRAINTS

As mentioned earlier, when the amplitudes of propagating waves are small, the investigation of the profile's shape and the form of the trajectories of its points is not important, as in the infinitesimal of equilibrium the shape of the surface is acceptably harmonic and trajectories of its points elliptic. However, there exist numerous technical applications where the oscillating profile performs the function of a transporting organ and the amplitudes of oscillations are relatively large if compared to the dimensions of the transported bodies (McCluskey et al., 1994; Moesner and Higudi, 1995; Hauser and Sommer, 1998). One of the examples of such systems is presented in Figure 1. The uncertainty of numerical simulations of such systems depends on the accuracy of mathematical models describing those systems. This fact can be illustrated by a simple mechanical system consisting of a small particle located on a propagating wave profile.

For simplicity, further analysis is performed in plane $x0y$ (Figure 1). Let a profile in the equilibrium state coincide with axis $0x$. Let a point of the profile in the equilibrium state $(x, 0)$ be translated to coordinates (u, v). Let this translation be time and coordinate sensitive

$$\begin{aligned} u &= x + \eta(x,t) \\ v &= \xi(x,t) \end{aligned} \tag{4}$$

where $\eta(x,t)$ and $\xi(x,t)$ are predefined functions. If

$$\eta(x,t) = a \sin(\omega t - kx)$$

$$\xi(x,t) = b\cos(\omega t - kx) \tag{5}$$

where a and b are constants, equation (4) will describe retrograde elliptical motion analogous to a traveling Rayleigh wave described by equation (1).

Let us denote the coordinates of the mass particle in plane $x0y$ as (u,v). The condition that the particle is located on the surface of the profile defined by equation (4) leads to the following constraint

$$v = \xi(x,t), \tag{6}$$

where x is to be found from the following equality in which u is given and x is the unknown:

$$x + \eta(x,t) = u. \tag{7}$$

In other words, the shape of the profile cannot be described explicitly. Really, the instantaneous shape of the Rayleigh surface wave is not a harmonic function. Nevertheless, the tangent to the surface of the profile at point u can be expressed explicitly

$$\tan\alpha = \frac{\xi'_x(x,t)}{1+\eta'_x(x,t)}, \tag{8}$$

where α denotes the angle between the tangent and the axis $0x$. By the way, when equation (5) is true, and $a = 1/k$; $kx - \omega t = \pi(2n+1)$; $n \in \mathbf{Z}$, then

$$|\tan\alpha| = \lim_{\substack{kx-\omega t\to \\ \pi(2n+1)}} \left| \frac{\frac{\partial\xi}{\partial x}}{1+\frac{\partial\eta}{\partial x}} \right| = \lim_{\substack{kx-\omega t\to \\ \pi(2n+1)}} \left| \frac{-kB(\sin(kx-\omega t))}{1+\cos(kx-\omega t)} \right| \approx \frac{kB\varepsilon}{\varepsilon^2} = \infty, \tag{9}$$

where ε is infinitesimal around $\pi(2n+1)$. Equation (9) represents the situation when the profile turns to be a propagating cyclone.

Let us denote the instantaneous velocities of the point of the profile in contact with the mass particle in the direction of axes $0x$ and $0y$ appropriately as $\dot{z}$ and $\dot{w}$, where dots represent full derivatives by t. These quantities can be calculated as

$$\begin{aligned} \dot{z} &= \eta'_t(x,t); \\ \dot{w} &= \xi'_t(x,t). \end{aligned} \tag{10}$$

It must be noted, that the expressions of $\dot{z}$ and $\dot{w}$ are not explicit, and the variable x in their expressions must be found from equation (7).

The condition that the mass particle will slide on the surface of the profile brings the following constraint into force

$$\tan\alpha = \frac{\dot{v} - \dot{w}}{\dot{u} - \dot{z}}, \tag{11}$$

where $\dot{u}$ and $\dot{v}$ are the instantaneous velocities of the mass particle in the direction of axes $0x$ and $0y$ appropriately. $\dot{v}$ can be expressed from equation (11):

$$\dot{v} = \left(\dot{u} - \eta_t'(x,t)\right) \frac{\xi_x'(x,t)}{1 + \eta_x'(x,t)} + \xi_t'(x,t)\,. \tag{12}$$

It can be noted again that x in equation (12) must be calculated from current u using relationship (7). Full differentiation by time of equation (7) leads to the relationship between $\ddot{z}$ and $\ddot{u}$, but the differentiation is not straightforward, as x is no longer a constant. As the mass particle slides on the surface of the profile, the coordinate of the origin of the surface point in contact with the mass particle changes. Step-by-step differentiation leads to (keeping in mind that $x_t' = \frac{\dot{u}-\eta_t'}{1+\eta_x'}$):

$$\begin{aligned}\ddot{v} &= \left(\ddot{u} - \eta_{xt}'' \frac{\dot{u} - \eta_t'}{1+\eta_x'} - \eta_{tt}''\right) \frac{\xi_x'}{1+\eta_x'} \\ &+ \frac{\dot{u} - \eta_t'}{\left(1+\eta_x'\right)^2} \left(\left(\xi_{xx}'' \frac{\dot{u}-\eta_t'}{1+\eta_x'} + \xi_{xt}''\right)\left(1+\eta_x'\right)\right. \\ &- \left.\xi_x' \left(\eta_{xx}'' \frac{\dot{u}-\eta_t'}{1+\eta_x'} + \eta_{xt}''\right)\right) + \xi_{xt}'' \frac{\dot{u}-\eta_t'}{1+\eta_x'} + \xi_{tt}''\,. \end{aligned} \tag{13}$$

Although the first impression can be that the relationship is quite complicated, analytical experiments with simple forms of functions η and ξ can exemplify its validity.

4. GOVERNING EQUATIONS OF MOTION

The relative sliding velocity of the mass particle on the surface of the profile is expressed as

$$v_{12} = (\dot{u} - \dot{z})\cos\alpha + (\dot{v} - \dot{w})\sin\alpha = \sqrt{1 + (\tan\alpha)^2}\,\left(\dot{u} - \eta_t'\right). \tag{14}$$

Then the linear friction force F between the mass particle and the profile takes the form

$$F = hv_{12}, \tag{15}$$

where h is the coefficient of viscous friction.

The condition of dynamic equilibrium leads to the following system of equations

$$\begin{cases} m\ddot{u} + N\sin\alpha + F\cos\alpha = 0 \\ m\ddot{v} + mg + F\sin\alpha = N\cos\alpha \end{cases} \tag{16}$$

where m is the mass of the particle, and N is the reaction force. Elementary transformations and substitutions lead to the expression of the governing equation of motion in the form

$$A(x,t)\cdot\ddot{u} + B(x,t)\cdot\dot{u} + C(x,t) + D(x,t)\cdot(\dot{u})^2 = 0, \tag{17}$$

where

$$
\begin{aligned}
A(x,t) &= 1+(\tan\alpha)^2, \\
B(x,t) &= \frac{h}{m}\left(1+(\tan\alpha)^2\right)+(2\xi''_{xt}-\eta''_{xt}\tan\alpha)\frac{\tan\alpha}{1+\eta'_x} \\
&\quad -(2\eta'_t\xi''_{xx}+\eta''_{xt}\xi'_x)\frac{\tan\alpha}{(1+\eta'_x)^2}+2\eta'_t\eta''_{xx}\xi'_x\frac{\tan\alpha}{(1+\eta'_x)^3}, \\
C(x,t) &= -\frac{h}{m}\eta'_t\left(1+(\tan\alpha)^2\right)+g\tan\alpha \\
&\quad +(\xi''_{tt}-\eta''_{tt}\tan\alpha)\tan\alpha+(\eta'_t\eta''_{xt}\tan\alpha-2\eta'_t\xi''_{xt})\frac{\tan\alpha}{1+\eta'_x} \\
&\quad +\left((\eta'_t)^2\xi''_{xx}+\eta'_t\eta''_{xt}\xi'_x\right)\frac{\tan\alpha}{(1+\eta'_x)^2}-(\eta'_t)^2\eta''_{xx}\xi'_x\frac{\tan\alpha}{(1+\eta'_x)^3}, \\
D(x,t) &= \left(\frac{\xi''_{xx}}{(1+\eta'_x)^2}-\frac{\xi'_x\eta''_{xx}}{(1+\eta'_x)^3}\right)\tan\alpha,
\end{aligned}
\tag{18}
$$

and $\tan\alpha$ is defined in equation (8).

If $\eta(x,t)=0$, the equation of motion can be simplified to the following form:

$$
\begin{aligned}
A(x,t) &= 1+(\xi'_x)^2; \\
B(x,t) &= \frac{h}{m}\left(1+(\xi'_x)^2\right)+2\xi''_{xt}\xi'_x; \\
C(x,t) &= g\xi'_x+\xi''_{tt}\xi'_x; \\
D(x,t) &= \xi''_{xx}\xi'_x; \\
\tan\alpha &= \xi'_x; \\
u &= x.
\end{aligned}
\tag{19}
$$

It can be noted that equation (17) is implicit. In fact, it contains two variables, u and x, which are cross-linked by relationship (8). If the ordinary differential equation (17) is solved using the time marching technique, the solution of equation (8) is necessary in every time step. As the unknown in equation (8) is x, not u, its solution poses considerable difficulties, first of all due to the non-uniqueness of the solution (the solution of equation (8) is unique only if $a < 1/k$). Application of computer algebra is also very much limited, and the equation can be solved using an iterative algorithm in every time step.

Nevertheless, equation (17) is a valuable product in the sense that the dynamics of a particle is considered on a profile that cannot be described explicitly. Moreover, it is a single-degree-of-freedom equation (not mentioning the hidden variable x).

When the reaction force

$$N = \frac{(m\ddot{v} + mg + F\sin\alpha)}{\cos\alpha} \tag{20}$$

turns out to be equal to zero, the particle loses its contact with the surface and its dynamics is governed by the following system of equations where u and v are independent variables:

$$\begin{cases} m\ddot{u} = 0; \\ m\ddot{v} + mg = 0. \end{cases} \tag{21}$$

5. DYNAMIC EQUILIBRIUM AND COEXISTING ATTRACTRORS

Natural dynamic equilibrium is the motion of a particle on the slope of a propagating wave with the velocity of its propagation (trivial regime of motion)

$$\begin{aligned} \ddot{u} &= 0, \\ \dot{u} &= \omega/k, \\ u &= \omega/k \cdot t + \psi, \end{aligned} \tag{22}$$

where ψ is a constant.

The conditions of existence and stability of the trivial regime of motion can be easily analyzed in the explicit form when $\eta(x,t) = 0$; $\xi(x,t) = b\cos(\omega t - kx)$. Then the condition of the existence takes the form

$$mg\sin\alpha + F = 0, \tag{23}$$

or, after elementary transformations,

$$(\tan\alpha)^2 + \frac{mgk}{h\omega}\tan\alpha + 1 = 0. \tag{24}$$

Equation (24) produces roots

$$(\tan\alpha)_{1,2} = -\frac{mgk}{2h\omega} \pm \sqrt{\left(\frac{mgk}{2h\omega}\right)^2 - 1}. \tag{25}$$

Thus, the necessary but not sufficient condition of the existence of the trivial regime of motion is

$$mg > 2h\frac{\omega}{k}. \tag{26}$$

Keeping in mind that $\tan\alpha = \xi'_x = -bk\sin(k\psi)$, equation (25) can be transformed to

$$\sin(k\psi_1) = \frac{mg}{2h\omega b} + \sqrt{\left(\frac{mg}{2h\omega b}\right)^2 - \frac{1}{b^2k^2}};$$

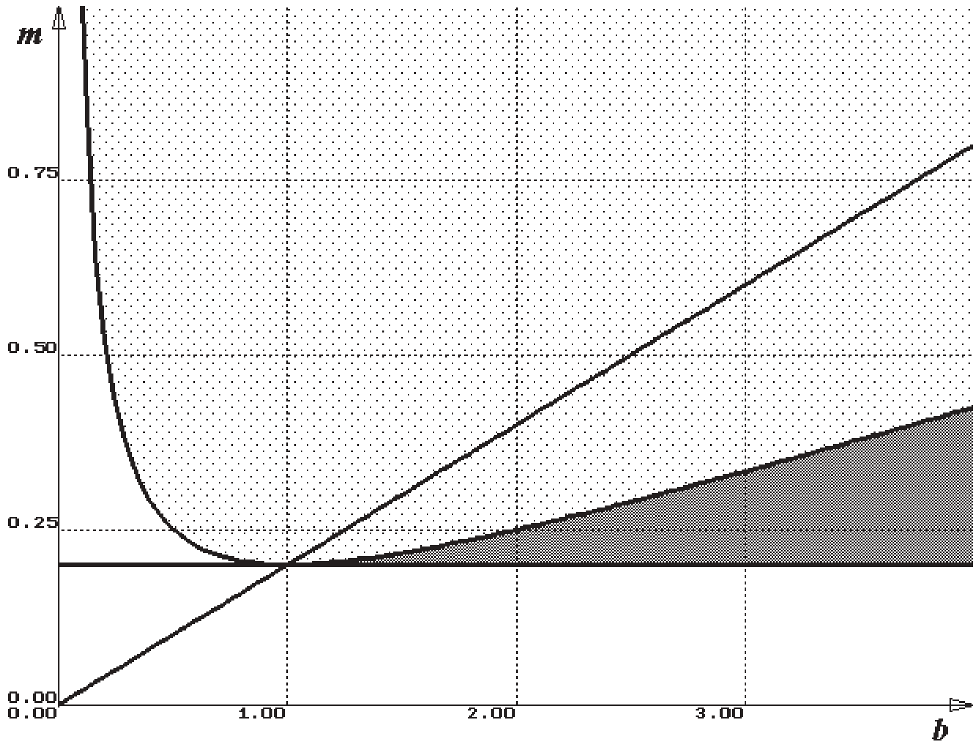

Figure 2. Region of existence of the trivial solutions: light-shaded zone, singular stable solutions; dark-shaded zone, multiple stable solutions.

$$\sin(k\psi_2) \quad = \quad \frac{mg}{2h\omega b} - \sqrt{\left(\frac{mg}{2h\omega b}\right)^2 - \frac{1}{b^2k^2}}. \tag{27}$$

If $\dfrac{mg}{2h\omega b} \geq 1$, then the equation for ψ_1 will have no solutions, and condition $\sin(k\psi_2) \leq 1$ will lead to

$$mg \geq \frac{h\omega\,(1 + b^2k^2)}{bk^2}. \tag{28}$$

Analogously, if $\dfrac{mg}{2h\omega b} < 1$, then the equation for ψ_2 will always have a solution, while the condition $\sin(k\psi_1) \leq 1$ will lead to inequality:

$$mg < \frac{h\omega\,(1 + b^2k^2)}{bk^2}. \tag{29}$$

It is important to note that the last condition means that there can exist multiple coexisting trivial solutions. Finally, the regions of the existence of trivial solutions are represented in Figure 2.

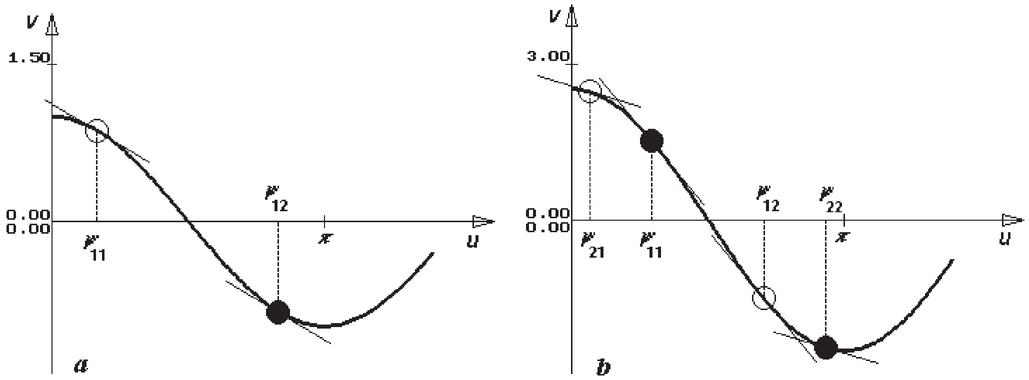

Figure 3. Dynamic equilibrium at: (a) $m = 0.25$, $g = 1$, $h = 0.1$, $b = 1$, $a = 0$, $\omega = 1$, $k = 1$; (b) $m = 0.25$, $g = 1$, $h = 0.1$, $b = 2.5$, $a = 0$, $\omega = 1$, $k = 1$. Black circles denote stable points; empty circles denote unstable points.

Equations (27) can produce a maximum of four sets of solutions

$$\begin{aligned}(\psi_{1,2})_1 &= \frac{1}{k}\arcsin\left(\frac{mg}{2h\omega b} \pm \sqrt{\left(\frac{mg}{2h\omega b}\right)^2 - \frac{1}{b^2k^2}}\right) + \frac{2\pi n}{k},\\ (\psi_{1,2})_2 &= \frac{\pi}{k} - (\psi_{1,2})_1 + \frac{4\pi n}{k},\end{aligned} \tag{30}$$

where $n \in \mathbf{Z}$.

The stability of the existing solutions is checked by the construction of variational equations in the infinitesimal around those solutions. If only ψ_2 exists, then $(\psi_2)_1$ is unstable and $(\psi_2)_2$ is stable. If both ψ_1 and ψ_2 exist, then $(\psi_1)_1$ and $(\psi_2)_2$ are stable, $(\psi_1)_2$ and $(\psi_2)_1$ are unstable. By the way, $(\psi_2)_1 < (\psi_1)_1 < (\psi_1)_2 < (\psi_2)_2$. This fact is illustrated in Figure 3.

Naturally, the trivial solution is not the only solution. When the condition of existence of trivial solutions is not satisfied, the system possesses different solutions than those described by equation (22). Moreover, solution (22) is not necessarily the only stable solution, even if the conditions of existence of that solution are satisfied. Different stable attractors can coexist. The reverse time marching technique from the surroundings of the unstable saddle point ψ_{11} (or two unstable saddle points ψ_{21} and ψ_{12}) enables the construction of attractor basin boundaries in phase plane $(\omega t - ku; \dot{u})$, which are presented in Figures 4 and 5. White zones denote the basins of attraction to the trivial solution; shaded zones denote the small average velocity solution; thick solid lines are reverse time marching trajectories from the unstable saddle point; thin solid lines are direct time marching trajectories from the unstable saddle point.

The effect of sensitivity of the solution and the shape of the small average velocity attractor can be clearly illustrated in the phase plane $(\dot{u}; \ddot{u})$ (Figure 6).

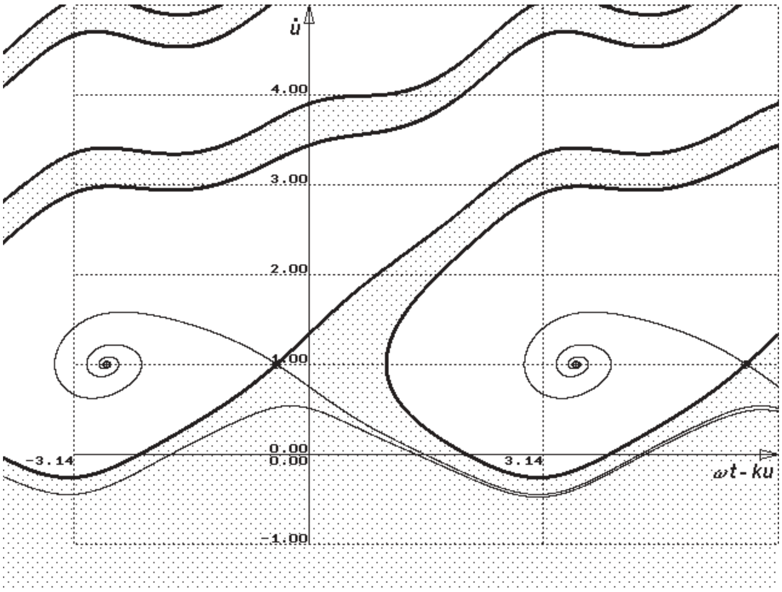

Figure 4. Basin boundaries of attractors at $h = 0.1$, $m = 0.5$, $g = 1$, $b = 0.5$, $a = 0$, $\omega = 1$, $k = 1$.

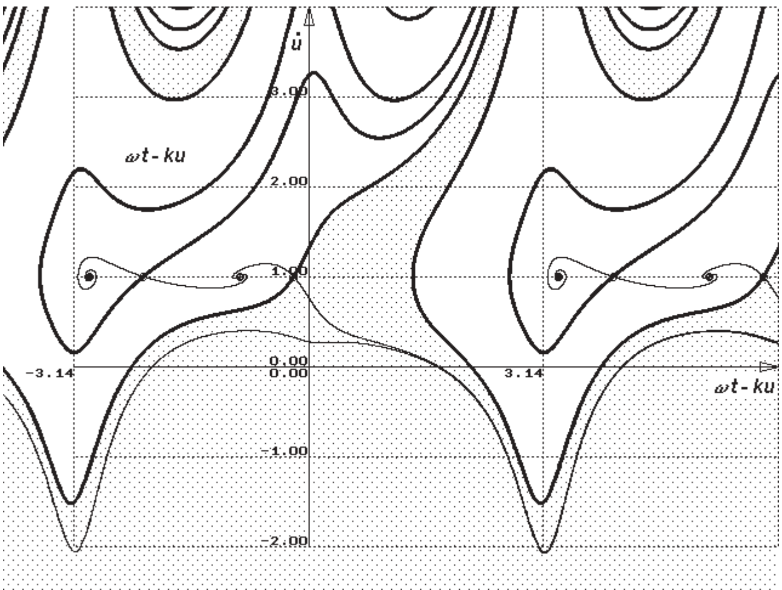

Figure 5. Basin boundaries of attractors at $h = 0.2$, $m = 0.5$, $g = 1$, $b = 2.5$, $a = 0$, $\omega = 1$, $k = 1$.

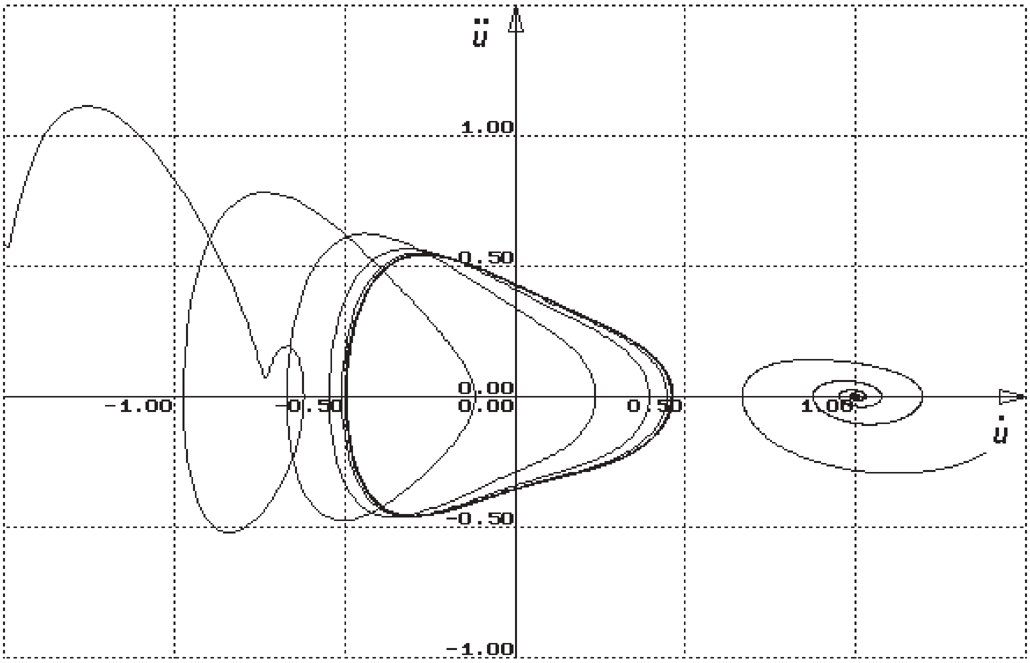

Figure 6. Transient solutions at $h = 0.1$, $m = 0.5$, $g = 1$, $b = 0.5$, $a = 0$, $\omega = 1$, $k = 1$.

It is interesting to note that the same effect of sensitivity to the initial conditions is valid also when $a > 0$, but the shape of the small average velocity attractor is different if compared to analogous attractor at $a = 0$. This is illustrated in Figure 7.

The points of dynamic equilibrium can be found also in case when $a > 0$, but only numerical techniques are used for this purpose. The black circle in Figure 8 denotes stable dynamic equilibrium. The system is integrated in time using the direct time marching technique until all transients fade out. It is much more difficult to find the unstable equilibrium, but the fact that it is located on the line $\dot{u} = \omega/k$ makes the problem easier (shooting of initial conditions and direct time marching technique is used).

The relationship between the average velocity and the amplitude of the traveling wave is presented in Figure 9. It can be seen that at certain values of b the dynamical system has two different attractors. At small amplitudes, the particle weight is two small to satisfy the conditions of existence of trivial regime of motion (those conditions are not the same as described in equation (30), as a is not zero). At a certain value of b the small average velocity attractor evolutes to a separatrix. At the limit value of b, the system stays infinitely long in the infinitesimal of the unstable saddle point. In some sense, this feature of the dynamics of the system reminds us of a nonlinear pendulum. The system possesses only a trivial regime of motion at higher b. It can be noted that $a = 0.7b$; so the transverse displacement is about one and a half times larger than the longitudinal displacement as mentioned previously in the description of a Rayleigh wave. Other parameters such as g, ω, and k are accepted to be non-dimensional for the simplicity of analysis. Further growth of b will lead to the jumping of the particle on the propagating profile.

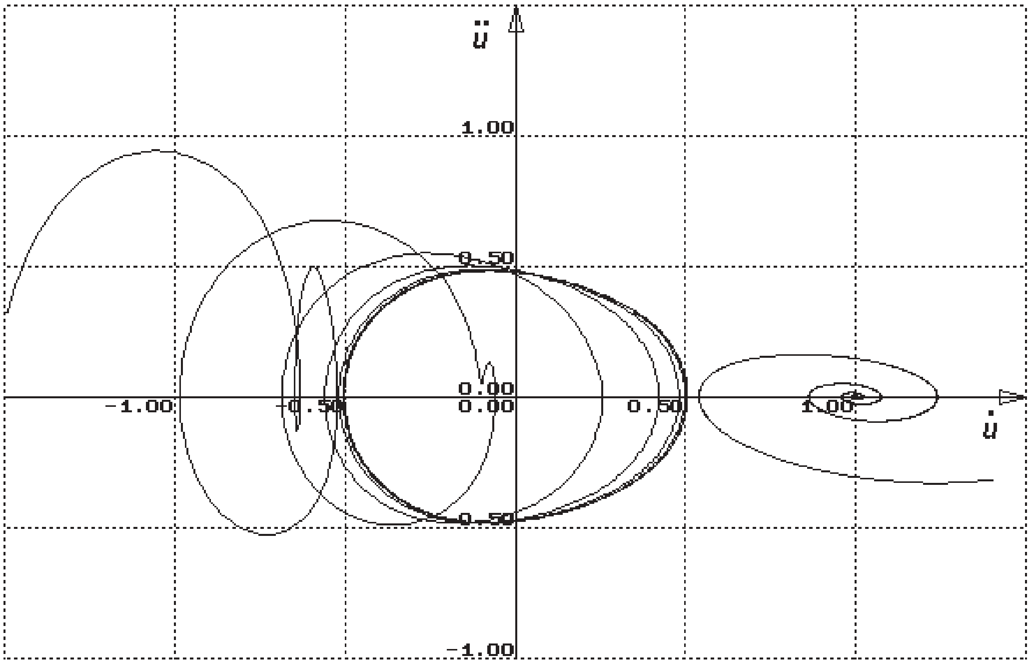

Figure 7. Transient solutions at $h = 0.1$, $m = 0.5$, $g = 1$, $b = 0.5$, $a = 0.4$, $\omega = 1$, $k = 1$.

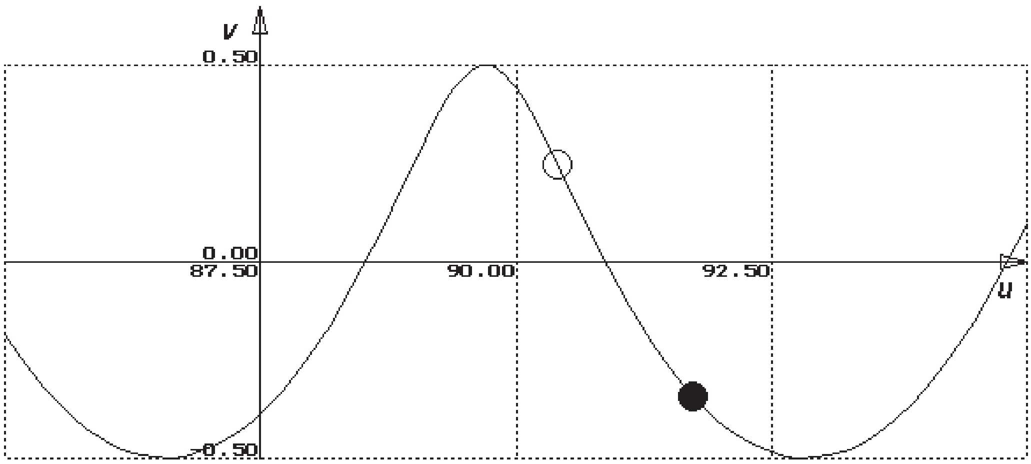

Figure 8. The shape of the profile and dynamic equilibrium at $h = 0.1$, $m = 0.5$, $g = 1$, $b = 0.5$, $a = 0.4$, $\omega = 1$, $k = 1$.

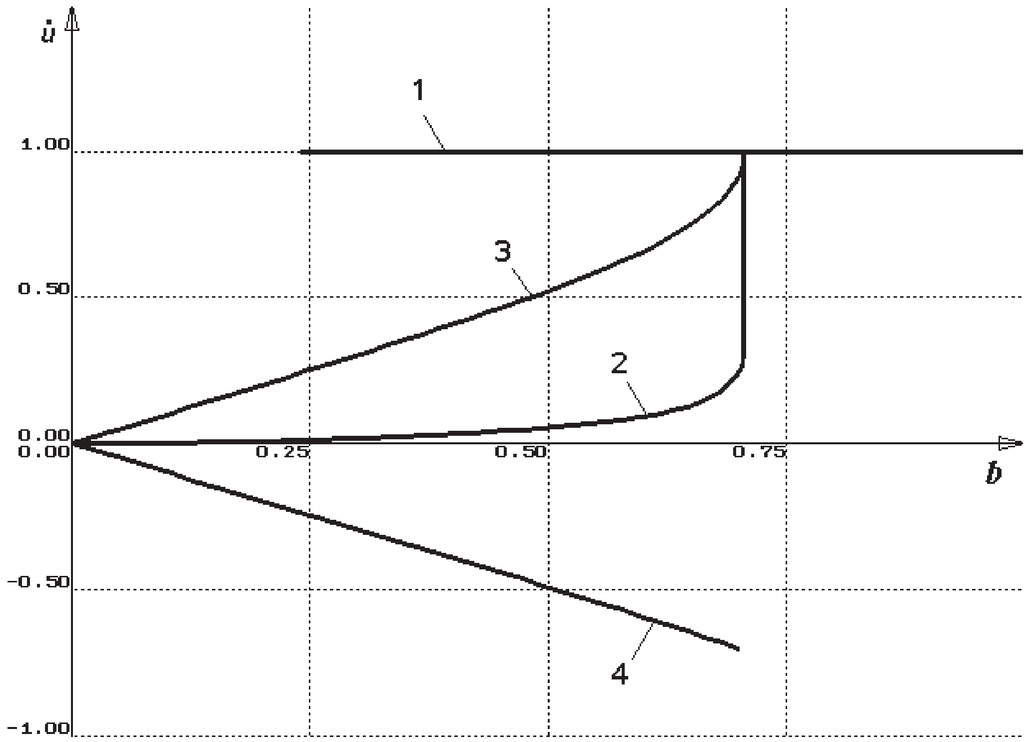

Figure 9. Relationship between the velocity of the particle and the amplitude of the traveling wave at $a = 0.7b$; $h = 0.1$, $m = 0.5$, $g = 1$, $\omega = 1$, $k = 1$. Line 1 represents the trivial regime of motion (dynamic equilibrium); line 2 represents the average velocity in a period of motion; lines 3 and 4 represent maximum and minimum velocities in a period.

6. DISCUSSION

The dynamics of a particle on the surface of an elastic body is a nonlinear problem, so such effects as the coexisting stable attractors should not be very astonishing. What is rather astonishing is that the dynamics of the analyzed system does resemble the motion of a nonlinear pendulum with external moment (Ragulskis, 2004). Many nonlinear features of the two physical systems described by different governing differential equations of motion are very much alike. The most attractive of these features is the coexistence of attractors; this fact enables the application of motion control strategy described in Ragulskis (2003). A small external impulse can bring the system to the basin of attraction of another regime of motion. Practically, this means that a small external impulse can bring the particle from the regime of motion with small average velocity into motion with the wave's velocity (trivial solution). In other words, the effectiveness of conveyance can be dramatically increased.

Another interesting feature is that the average velocity of a particle in the non-trivial regime of motion can be positive, although the design of such mechanisms as ultrasonic motors or feeding instruments (Figure 1) is based on the opposite effect. This should not be astonishing, as the transported bodies usually do contact only with the upper regions of the deformed boundaries in the mentioned systems. The retrograde elliptic motion transports those bodies in the reverse direction. In our model the particle slides all through the surface without losing contact with the surface (if only it does not jump off the surface as described in equations (20) and (21)).

The acquired results are in some sense promising for the analysis of more complex systems as described in Figure 1. If the dynamics of a system where the transported element is a deformable body is also sensitive to the initial conditions, the analogous control strategy based on small external impulses can be applied, leading to far more effective modes of operation. This is the object of future research.

REFERENCES

Achenbach, J. D., 1984, *Wave Propagation in Elastic Solids*, Elsevier, New York.

Benisti, D. and Escande, D. F., 1997, "Explicit reduction of N-body dynamics to self-consistent particle-wave interaction," *Physics of Plasmas* **4**, 1576–1581.

Elskens, Y., Guyomarch, D., and Firpo, M. C., 1998, "Phase space dynamics and wave – particle interaction," *Physics Magazine* **20**, 193–203.

Hauser, G. and Sommer, K., 1998, "Plug flow type pneumatic conveying of abrasive products in food industry," *Journal of Powder and Bulk Solids Technology* **12**, 511–519.

Hui, L. and Tomita, Y., 2000, "A numerical simulation of swirling flow pneumatic conveying in a horizontal pipeline," *Particulate Science and Technology: An International Journal* **18(4)**, 275–292.

Jacobsen, M. L., McCluskey, D. R., Easson, W. J., and Greated, C. A., 1994, "Pneumatic particle conveyance in a pipe bend: simultaneous two phase PIV measurements of the slip velocity between the air and particle phases," in *Proceedings of the 7th International Symposium on Applications of Laser Techniques to Fluid Mechanics*, Lisbon, Portugal.

Landau, L. D. and Lifschitz, E. M., 1986, *Theory of Elasticity*, 3rd edition, Pergamon Press, Oxford.

McCluskey, D. R., Hind, A. K., and Greated, C. A., 1994, "Development and application of a simultaneous two phase PIV system for analysis of air-particle flow fields," in *Optical Methods and Data Processing in Heat and Fluid Flow*, City University, London, pp. 99–110.

Moesner, F. and Higudi, T., 1995, "Devices for particle handling by an AC electrical field," in *Proceedings of IEEE Workshop on Micro Electro Mechanical Systems*, Amsterdam, the Netherlands, pp. 66–71.

Ragulskis, M., 2004, "Coexisting attractors and their control in a rotary motion transfer mechanics," *Journal of Vibration and Control* **10**, 101–113.

Tokar, A. M. and Ulitko, A. F., 1984, "Motion of material particle under the influence of elastic oscillations of a surface of body," *Herald of Academy of Sciences of Ukraine* **A7**, 46–49.